Decentralized Bilateral Risk-based Self-healing Strategy for Power Distribution Network with Potentials from Central Energy Stations

Chaoxian Lv, Rui Liang, and Yuanyuan Chai

Abstract—**Owing to potential regulation capacities from flexible resources in energy coupling, storage, and consumption links, central energy stations (CESs) can provide additional support to power distribution network (PDN) in case of power disruption. However, existing research has not explicitly revealed the emergency response of PDN with leveraging multiple CESs. This paper proposes a decentralized self-healing strategy of PDN to minimize the entire load loss, in which multi-area CESs' potentials including thermal storage and building thermal inertia, as well as the flexible topology of PDN, are reasonably exploited for service recovery. For sake of privacy preservation, the co-optimization of PDN and CESs is realized in a decentralized manner using adaptive alternating direction method of multipliers (ADMM). Furtherly, bilateral risk management with conditional value-at-risk (CVaR) for PDN and risk constraints for CESs is integrated to deal with uncertainties from outage duration. Case studies are conducted on a modified IEEE 33-bus PDN with multiple CESs. Numerical results illustrate that the proposed strategy can fully utilize the potentials of multi-area CESs for coordinated load restoration. The effectiveness of the performance and behaviors' adaptation against random risks is also validated.**

Index Terms—**Power distribution network (PDN), central energy station (CES), bilateral risk management, self-healing, alternating direction method of multipliers (ADMM).**

NOMENCLATURE

A. Symbols

$B_{t'}$	Probability with outage duration t'
C, H	Cooling and heating power
C_{air}	Specific heat capacity of air
$C_{t,n}^{\text{in}}$	Injected cooling for building
E^{E}, E^{C}	Unit penalty costs for electricity and cooling loads
F_n	Surface area of building
f_s	Objective value
I, l	Current magnitude and its square of branch
K_n	Equivalent heat dissipation coefficient
N_s	Number of scenarios
P, Q	Active and reactive power
$\boldsymbol{P}_{\text{e}}$, $\boldsymbol{Q}_{\text{e}}$	Active and reactive injections into power distribution network (PDN) of coupling points
$\boldsymbol{P}_{\text{ces}}$, $\boldsymbol{Q}_{\text{ces}}$	Active and reactive outputs of gas turbines (GTs) in central energy stations (CESs)
p_s	Probability of scenario s
p_t	Comprehensive probability of period t
r, x	Resistance and reactance of branch
S	Inverter capacity
T	Indoor temperature of buildings
$T_{t,\text{out}}$	Outdoor temperature
T_{ref}	Reference indoor temperature
t_{in}	The minimum value of inevitable outage duration
t_{out}	Outage duration time
V, v	Voltage magnitude and its voltage square of bus
V_0	System reference voltage
V_n	Volume of building
W	Cooling energy stored
$\boldsymbol{Z}_p$, $\boldsymbol{Z}_q$	Consensus variables

B. Greek Symbols

α	Binary variable (1: branch is connected; 0: otherwise)
β_{ij}	Binary variable (1: node j is the parent of bus i; 0: otherwise)
δ	Power factor of gas turbines
Δt	Scheduling interval
ΔT	Ramping limit
ε, λ	Heat loss rate and load recovery coefficient

Manuscript received: July 21, 2022; revised: October 25, 2022; accepted: December 26, 2022. Date of CrossCheck: December 26, 2022. Date of online publication: January 27, 2023.

This work was financially supported by the Fundamental Research Funds for the Central Universities (No. 2021QN1066).

C. Lv and R. Liang are with School of Electrical Engineering, China University of Mining and Technology, Xuzhou, China (e-mail: chaoxianlv@163.com; liangrui@cumt.edu.cn).

Y. Chai (corresponding author) is with School of Electrical Engineering, Hebei University of Technology, Tianjin, China (e-mail: yychai@hebut.edu.cn).

DOI: 10.35833/MPCE.2022.000436

ζ	Value at risk
η	Efficiency of gas-driven device
$\boldsymbol{\lambda}_{e,p}$, $\boldsymbol{\lambda}_{e,q}$	Vectors of Lagrangian multipliers for PDN
$\boldsymbol{\lambda}_{\text{ces},p,n}$, $\boldsymbol{\lambda}_{\text{ces},q,n}$	Vectors of Lagrangian multipliers for CESs n
μ, σ	Step size adjustment parameters
π_s, π_t	Non-negative values
ρ	Penalty parameter
ρ_{air}	Density of air
τ	Heat-electricity ratio
φ	Confidence level
ω	Weight factor of risk
Ω	Set of specified elements

C. Superscripts

HP, WC, CWT, GT, AC	Heat pump, water-cooled chiller, cold water tank, gas turbine, and absorption chiller
k	Index of iteration number
L, TL	Load and tie line
max, min	The maximum and minimum values
S, R	Cooling storage and releasing

D. Subscripts

br, b	Branch and bus
i, j	Indices of buses
ij, jh	Indices of branches
n, s	Indices of CESs and scenarios
t	Index of time periods
tie, v	Tie switch and voltage support bus

I. Introduction

THE energy dilemma and environmental pollution issues have expedited the revolution of energy utilization [1], [2]. Electricity-gas energy system (EGES), in which energies are distributed by power distribution network (PDN) and natural gas system and end-consumers are fed by central energy stations (CESs), has been widely spread to achieve high-efficiency and low-carbon operation [3]. Due to the existence of flexible resources in energy coupling, storage and consumption links, CESs have become the key points for multi-energy coordination and systematic facilitation [4]. And the regulation potential from CESs can provide additional support for the operation of PDNs in normal and extreme cases [5].

Recently, frequent occurrences of emergencies such as natural disasters and hostile attacks bring out tremendous operation loss to energy system, and these events have the characteristics of low probability and large destruction [6], [7]. Especially, the PDN is more likely to suffer extreme power outages due to the ubiquity of vulnerable electricity infrastructures [8]. Thus, adequate adaption and self-healing response capacity in case of outages are essential for the secure and reliable operation of PDN [9].

Significant efforts have been conducted on the self-healing scheduling of PDN under extreme events. The utilization of various controllable resources such as distributed generations (DGs), network reconfiguration, and demand-side approaches can contribute to the service recovery effect [10]. With the support of DGs and flexible topology of distribution networks, a service restoration strategy is employed in [11] to restore out-of-service loads as much as possible. Reference [12] proposes a supply restoration strategy for active distribution network with soft open points (SOPs), in which the sequential operations of SOP control mode and switching motion are coordinated. Considering the time-series of DGs, energy storage systems (ESSs), and loads, [13] constructs a SOP-based island partition model for load recovery. Reference [14] applies a multi-fault rush repairing strategy to distribution network for minimizing the outage loss and rush repairing time. A synchronous fault location, fault isolation, and service restoration method is proposed in [15], with the post-event recovery ability improved. Considering the threat of ice disaster, a resilience strategy is proposed in [16] by proactive network reconfiguration, with the survivability under disasters improved. Multiple sources including DGs and microgrids are coordinated in [17] for the restoration of critical loads after blackouts, and the restoration problem is solved by two-stage determination of post-event topology and source-load states. By the inclusion of demand response (DR) for varying the load profiles, the service restoration level is significantly leveraging in [18].

As energy systems are undergoing a transition from separated power supply pattern to multi-energy and multi-link collaboration, the coordination potentials of heterogeneous resources for electricity service recovery will be exploitable [19]. Especially, the coupling between electricity and natural gas is progressively increasing due to the widespread application of gas turbines (GTs) and electricity-gas CESs [20], [21]. Along with the flexibility promotion for fault restoration, challenges are arising parallelly on account of interdependence and constraint aggravation [22]. With the interactive support of electricity and natural gas infrastructures, the damages caused by attackers are effectively weakened with three-stage defender-attacker-defender strategy [23], [24]. Reference [25] constructs a multi-energy coordinated load restoration strategy for urban integrated energy system, in which the minimum spanning tree method is used to decompose the distribution network into a multi-island mode for the prioritized recovery of critical loads. To increase the emergency response capacities of power grid, [26] conducts an electricity-gas synergy planning with replacing certain power lines with natural gas transportation system. By exploiting the emergency support of gas/electricity, thermal storages, and building demand response, a multi-stage resilience scheduling with multi-level reserve is investigated in [27]; the critical loads in PDN can be strictly guaranteed. Reference [28] proposes a dynamic recovery strategy for integrated distribution networks, in which available resources including GTs and mobile storages are managed collaboratively to improve the amount of restored electricity loads.

With the optimal operation of combined heat and power (CHPs), a microgrid formation model of electricity-gas system is presented in [29] for resilience improvement.

The above researches mainly focus on the centralized scheduling manner that ignores the obstacles of information exchange. Different utilities may have autocephalous energy management systems (EMSs) and they are usually operated independently with privacy-preserving [30]. Thus, the decentralized scheduling approach, which can decompose original problem into some sub-problems with limited information sharing, has become an applicable choice to realize collaborative optimization [31]. To convert original centralized operation problem into a decentralized mode, several methods including augmented Lagrangian relaxation (ALR), alternating direction method of multipliers (ADMM), and analytical target cascading (ATC) have been developed [32], [33]. Due to preferable convergence performance and extendable decomposing structure, ADMM is widely adopted for solving multi-system co-operation problems [34]. In [35], a decentralized demand response management for industrial park energy system is conducted using the ADMM algorithm. The co-optimization of multi-area integrated electricity-gas systems is realized through ADMM algorithm in [36], and the convergence and accuracy are validated. The optimization process of each subsystem, i.e., electric distribution system, natural gas system, and energy hub systems, is conducted separately by utilizing consensus-based ADMM algorithm in [37]. For the load restoration problem of integrated power distribution and gas systems, [38] uses a consensus-based ADMM algorithm to fulfill scheduling in a distributed manner, with excessive information exchange avoided and utility privacy preserved.

Moreover, extra risks will be evoked regarding various uncertainties, which may derive from renewable energy sources (RESs), multiple demands, and some others. To decrease the negative influence, handling methods such as robust optimization [39], stochastic optimization [40], and chance-constrained programming [41] can be employed for better adaptability to uncertain factors. Conditional value-at-risk (CVaR) is a concept derived from economic field to measure the loss risk of investments, and it has significant application value for risk management on the planning and operation of PDN, microgrid, and integrated energy systems [42]. For the trade-off between risk and cost under source-load variations, [43] carries out CVaR-based investment-operation planning for multi-energy microgrid, which can provide investment recommendations for decision-makers. A CVaR-averse penalty of voltage violation is integrated into the chance-constrained optimal power flow in [44], with better voltage security guaranteed. To solve the risk caused by fluctuations from RESs and loads, CVaR is introduced into the reserve decision of islanded micrgorid for the coordination of operation security and economy in [45]. Facing various uncertainties including solar, load, and day-ahead price, [46] proposes a risk management model for power, heat, and hydrogen system based on CVaR, and operator's behaviors against random risks are contrastively discussed. As an effective means for risk management, the CVaR indices have not been well utilized in the self-healing scheduling of PDN under uncertainties. It should be noted that conventional self-healing scheduling is usually developed based on the deterministic estimated duration time after fault isolation; in reality, the fault duration is affected by various factors such as disaster situation and rush repair time, resulting in uncertainty of outage duration and operation risk of multiple coupling periods in PDN.

To the best of our knowledge, the uncertainties from outage duration have not attracted much attention in the service recovery of PDN. Facing indeed existing duration disturbance in PDN, it still lacks efficient self-healing strategy due to the time-series relevance of system status for uncertain scenarios. Especially, with deep coupling between PDN and CESs, the auxiliary service potentials of CESs for emergency response need to be well exploited; meanwhile, the integration of CESs raises the difficulty of reasonable risk-based restoration due to the requirements of multi-energy coordination and spatio-temporal resource utilization. Furthermore, the operations of PDN and CESs are often independent along with private information preserving; the optimal self-healing strategy considering endogenous uncertainty from outage duration is more challenging.

To deal with the above issues, this paper proposes a decentralized risk-based self-healing strategy for PDN considering the support of multiple CESs. The main contributions are summarized as follows.

1) A self-healing recovery strategy for PDN is proposed considering topology reconfiguration and multiple regulation potentials of multi-area CESs. For dispersive CESs, emergency response from GTs and thermal storage, as well as building thermal inertia are well coordinated for load restoration. Furthermore, the model is tackled as a mixed-integer second-order cone programming (MISOCP) problem.

2) Bilateral risk management with CVaR assessment for PDN and margin constraints for CESs is employed to cope with operation risks caused by uncertain outage duration. CVaR criteria are introduced to measure the load shedding risk of PDN while guaranteeing the supply of CESs within permissible margin for risk controllability. Better risk management effects are realized.

3) The self-healing strategy is conducted in a decentralized manner, in which consensus-based ADMM algorithm is adopted for reducing information exchange and preserving privacy between PDN and CESs. Meanwhile, the iteration process is expedited by adaptive ADMM algorithm, showing better convergence performance.

The remainder of this paper is organized as follows. Section II builds the mathematical model of system operation, as well as the conic relaxation method. Section III describes the bilateral risk-based self-healing scheduling strategy. The solution methodology of decentralized risk-based self-healing scheduling is presented in Section IV. Case studies are conducted in Section V to verify the performance of the proposed strategy. Finally, conclusions are drawn in Section VI.

II. Mathematical Model of System Operation

A. Constraints of PDN

1) Power Flow Constraints

The DistFlow branch model with considering flexible topology is adopted to describe the PDN. Equations (1) and (2) denote the active and reactive power balances of node j at time t. And the branch current magnitude can be obtained by (3). Besides, the active and reactive power injections of node j at time t are described in (4) and (5). Considering network reconfiguration characteristic, the Ohm's law of branch ij at time t is denoted in (6) and (7); and (8)-(10) are supplemented for guaranteeing accuracy, where M is a sufficiently large constant.

$$\sum_{ij \in \Omega_{\text{br}}} (P_{t,ij} - r_{ij} I_{t,ij}^2) + P_{t,j} = \sum_{jh \in \Omega_{\text{br}}} P_{t,jh} \tag{1}$$

$$\sum_{ij \in \Omega_{\text{br}}} (Q_{t,ij} - x_{ij} I_{t,ij}^2) + Q_{t,j} = \sum_{jh \in \Omega_{\text{br}}} Q_{t,jh} \tag{2}$$

$$V_{t,i}^2 I_{t,ij}^2 = P_{t,ij}^2 + Q_{t,ij}^2 \tag{3}$$

$$P_{t,j} = -P_{t,n}^{\text{TL}} - \lambda_{t,j} P_{t,j}^{\text{L}} \quad n \in \Omega_{\text{b},j}^{\text{CES}} \tag{4}$$

$$Q_{t,j} = Q_{t,n}^{\text{GT}} - \lambda_{t,j} Q_{t,j}^{\text{L}} \quad n \in \Omega_{\text{b},j}^{\text{CES}} \tag{5}$$

$$V_{t,i}^2 - V_{t,j}^2 - 2(r_{ij} P_{t,ij} + x_{ij} Q_{t,ij}) + (r_{ij}^2 + x_{ij}^2) I_{t,ij}^2 + M(1 - \alpha_{ij}) \ge 0 \tag{6}$$

$$V_{t,i}^2 - V_{t,j}^2 - 2(r_{ij} P_{t,ij} + x_{ij} Q_{t,ij}) + (r_{ij}^2 + x_{ij}^2) I_{t,ij}^2 - M(1 - \alpha_{ij}) \le 0 \tag{7}$$

$$-M\alpha_{ij} \le P_{t,ij} \le M\alpha_{ij} \tag{8}$$

$$-M\alpha_{ij} \le Q_{t,ij} \le M\alpha_{ij} \tag{9}$$

$$0 \le i_{t,ij} \le M\alpha_{ij} \tag{10}$$

2) Topology Constraints

The radical topology should be maintained in the formed islands, which is described as:

$$\alpha_{ij} = \beta_{ij} + \beta_{ji} \quad ij \in \Omega_{\text{br}} \tag{11}$$

$$\sum_{ij \in \Omega_{\text{br}}} \beta_{ij} = 1 \quad \forall i \in \Omega_{\text{b}} / \Omega_{\text{v}} \tag{12}$$

$$\sum_{ij \in \Omega_{\text{br}}} \beta_{ij} = 0 \quad \forall i \in \Omega_{\text{v}} \tag{13}$$

$$V_{t,i} - V_0 \ge -M \sum_{ij \in \Omega_{\text{br}}} \beta_{ij} \tag{14}$$

where V_0 is the system reference voltage. Equation (11) represents the relationship between branch connect state and flow direction; (12) and (13) denote that there is no parent bus for root node and merely one node is permitted to serve as the parent of other nodes; and (14) is to constrain the voltage of root bus.

3) Security Constraints

The security constraints are to restrict the magnitudes of bus voltage and line current.

$$(V^{\min})^2 \le V_{t,i}^2 \le (V^{\max})^2 \tag{15}$$

$$I_{t,ij}^2 \le (I_{ij}^{\max})^2 \tag{16}$$

B. Constraints of CES

This research mainly focuses on the self-healing scheduling for space cooling and electricity during the cooling period. And the cooling devices can be divided into electricity-driven and gas-driven categories.

1) Electricity-driven Devices

Popular electricity-driven devices include ground source heat pump (HP), conventional water-cooled chiller (WC), and cold water tank (CWT).

The mathematical model of HP is depicted in (17) and (18), where COP denotes coefficient of performance.

$$C_n^{\text{HP,min}} \le C_{t,n}^{\text{HP}} \le C_n^{\text{HP,max}} \tag{17}$$

$$P_{t,n}^{\text{HP}} = C_{t,n}^{\text{HP}} / COP_n^{\text{HP}} \tag{18}$$

The operation constraints of WC are given in (19) and (20).

$$C_n^{\text{WC,min}} \le C_{t,n}^{\text{WC}} \le C_n^{\text{WC,max}} \tag{19}$$

$$P_{t,n}^{\text{WC}} = C_{t,n}^{\text{WC}} / COP_n^{\text{WC}} \tag{20}$$

CWTs can store the cooling energy from HPs and WCs, and the energy storage constraints, cooling-storage constraints, and capacity constraints are formulated as follows:

$$W_{t,n}^{\text{CWT}} = (1 - \varepsilon_n^{\text{CWT}}) W_{t-1,n}^{\text{CWT}} + C_{t,n}^{\text{CWT,S}} \Delta t - C_{t,n}^{\text{CWT,R}} \Delta t \tag{21}$$

$$C_{t,n}^{\text{HP}} + C_{t,n}^{\text{WC}} \ge C_{t,n}^{\text{CWT,S}} \tag{22}$$

$$0 \le W_{t,n}^{\text{CWT}} \le W_n^{\text{CWT,max}} \tag{23}$$

2) Gas-driven Devices

Gas-driven devices can be GT and absorption chiller (AC). GTs burn natural gas with electricity and heating generation, and electricity and heating have a certain ratio relationship, as shown in (24) and (25). And (26) presents the constraints of output power.

$$P_{t,n}^{\text{GT}} = \eta_n^{\text{GT}} F_{t,n}^{\text{GT}} \tag{24}$$

$$H_{t,n}^{\text{GT}} = \tau_n^{\text{GT}} P_{t,n}^{\text{GT}} \tag{25}$$

$$0 \le P_{t,n}^{\text{GT}} \le P_n^{\text{GT,max}} \tag{26}$$

In case of disruption at the root node of PDN, complete energy loss will occur. Facing this, both active and reactive power supports should be carried out for effective fault restoration. As the coupling point of PDN and natural gas system, converter-based GTs in CESs can serve as controllable distributed generators to provide active and reactive support when electricity emergency takes place [47]. And the power factor of GT should be larger than the minimum allowed value, which can be represented in the form of (27). Furtherly, the converter capacity of GT is constrained in (28).

$$-\frac{P_{t,n}^{\text{GT}} \sqrt{1 - (\delta_n^{\min})^2}}{\delta_n^{\min}} \le Q_{t,n}^{\text{GT}} \le \frac{P_{t,n}^{\text{GT}} \sqrt{1 - (\delta_n^{\min})^2}}{\delta_n^{\min}} \tag{27}$$

$$\sqrt{(P_{t,n}^{\text{GT}})^2 + (Q_{t,n}^{\text{GT}})^2} \le S_n^{\text{GT}} \tag{28}$$

The output power constraints, absorbed power, as well the maximum output constraints of AC are shown as follows:

$$C_{t,n}^{\text{AC}} = COP_n^{\text{AC}} \cdot H_{t,n}^{\text{AC}} \tag{29}$$

$$H_{t,n}^{\text{AC}} \le H_{t,n}^{\text{GT}} \tag{30}$$

$$0 \le C_{t,n}^{\text{AC}} \le C_n^{\text{AC,max}} \tag{31}$$

3) Thermal Inertia Model of Buildings

The thermal inertia characteristic of buildings will provide more flexibilities for system operation, and buildings can be regarded as virtual storages. The mathematical thermal inertia model of buildings in the cooling season can be stated as [48]:

$$\frac{T_{t,n}-T_{t-1,n}}{\Delta t}=\frac{(T_{t,\mathrm{out}}-T_{t-1,n})K_nF_n-C_{t,n}^{\mathrm{in}}}{C_{\mathrm{air}}\rho_{\mathrm{air}}V_n} \tag{32}$$

4) Power Balance Constraints

The energy supply-demand balances should be ensured every time, and electricity and cooling balances in CESs are expressed as:

$$P_{t,n}^{\mathrm{TL}}+P_{t,n}^{\mathrm{GT}}=P_{t,n}^{\mathrm{HP}}+P_{t,n}^{\mathrm{WC}} \tag{33}$$

$$C_{t,n}^{\mathrm{HP}}+C_{t,n}^{\mathrm{WC}}+C_{t,n}^{\mathrm{AC}}-C_{t,n}^{\mathrm{CWT,S}}+C_{t,n}^{\mathrm{CWT,R}}=C_{t,n}^{\mathrm{in}} \tag{34}$$

C. Convex Conversion of System Operation

Lots of nonconvex terms exist in the operation model. To expedite the solution, the nonconvex model is converted into an MISOCP formulation.

1) PDN

Auxiliary variables $l_{t,ij}$ and $v_{t,i}$ are introduced to replace $I_{t,ij}^2$ and $V_{t,i}^2$. Thus, (1), (2), (6), (7), (15), and (16) can be linearized:

$$\sum_{ij\in\Omega_{\mathrm{br}}}(P_{t,ij}-r_{ij}l_{t,ij})+P_{t,j}=\sum_{jh\in\Omega_{\mathrm{br}}}P_{t,jh} \tag{35}$$

$$\sum_{ij\in\Omega_{\mathrm{br}}}(Q_{t,ij}-x_{ij}l_{t,ij})+Q_{t,j}=\sum_{jh\in\Omega_{\mathrm{br}}}Q_{t,jh} \tag{36}$$

$$v_{t,i}-v_{t,j}-2(r_{ij}P_{t,ij}+x_{ij}Q_{t,ij})+(r_{ij}^2+x_{ij}^2)l_{t,ij}+M(1-\alpha_{ij})\geq 0 \tag{37}$$

$$v_{t,i}-v_{t,j}-2(r_{ij}P_{t,ij}+x_{ij}Q_{t,ij})+(r_{ij}^2+x_{ij}^2)l_{t,ij}-M(1-\alpha_{ij})\leq 0 \tag{38}$$

$$(V^{\min})^2\leq v_{t,i}\leq (V^{\max})^2 \tag{39}$$

$$l_{t,ij}\leq (I_{ij}^{\max})^2 \tag{40}$$

For (3), it can be further relaxed as a standard second-order cone constraint, which can be expressed as:

$$\left\|[2P_{t,ij}\quad 2Q_{t,ij}\quad l_{t,ij}-v_{t,i}]^{\mathrm{T}}\right\|_2\leq l_{t,ij}+v_{t,i} \tag{41}$$

2) CES

For GT operation in case of electricity emergency, (28) can be converted as a rotating cone constraint:

$$(P_{t,n}^{\mathrm{GT}})^2+(Q_{t,n}^{\mathrm{GT}})^2\leq 2\frac{S_n^{\mathrm{GT}}}{\sqrt{2}}\frac{S_n^{\mathrm{GT}}}{\sqrt{2}} \tag{42}$$

After convex relaxation and linearization, the original operation model is reformulated as an MISOCP model, which can be effectively solved by mature commercial solver.

III. Bilateral Risk-based Self-healing Scheduling

In the section, the bilateral risk-based self-healing model is introduced to realize service recovery and risk measures.

A. Objective Function

The objective function F is to minimize the load losses of PDN and CESs, which is:

$$\min F=\sum_{t=1}^{t_{\mathrm{out}}}p_t(E^{\mathrm{E}}L_t^{\mathrm{E,NS}}+E^{\mathrm{C}}L_t^{\mathrm{C,NS}})\Delta t \tag{43}$$

$$L_t^{\mathrm{E,NS}}=\sum_{i\in\Omega_{\mathrm{b}}}(1-\lambda_{t,i})P_{t,i}^{\mathrm{L}} \tag{44}$$

$$L_t^{\mathrm{C,NS}}=\sum_{n\in\Omega_{\mathrm{CES}}}\left|T_{t,n}-T_{\mathrm{ref}}\right|C_{\mathrm{air}}\rho_{\mathrm{air}}V_n/\Delta t \tag{45}$$

p_t can be calculated as:

$$p_t=\begin{cases}1 & t<t_{\mathrm{in}}\\ \dfrac{A_t}{\sum\limits_{t=t_{\mathrm{in}}+\Delta t}^{t_{\mathrm{out}}}A_t} & \text{others}\end{cases} \tag{46}$$

where A_t equals $\sum\limits_{t'=t}^{t_{\mathrm{out}}}B_{t'}$.

B. Bilateral Risk-based Scheduling

1) CVaR-based Risk Management for PDN

The general expression of CVaR model can be described as follows [49]:

$$\min\left(\zeta+\frac{1}{1-\varphi}\sum_{s=1}^{N_s}p_s\pi_s\right) \tag{47}$$

$$f_s-\zeta\leq\pi_s \tag{48}$$

$$\pi_s\geq 0 \tag{49}$$

where π_s is greater than $f_s-\zeta$ in scenario s.

Based on the above CVaR theory and system optimization model, the risk-management model of self-healing strategy can be reformulated as (50).

$$\min\left\{(1-\omega)F+\omega\left(\zeta+\frac{1}{1-\varphi}\sum_{t=t_{\mathrm{in}}+\Delta t}^{t_{\mathrm{out}}}p_t\pi_t\right)\right\} \tag{50}$$

Except for the original constraints for system operation, the following constraints are supplemented to risk management model.

$$L_t^{\mathrm{E,NS}}-\zeta\leq\pi_t\quad\forall t>t_{\mathrm{in}} \tag{51}$$

$$\pi_t\geq 0 \tag{52}$$

In general, we describe the strategy with $\omega>0.5$ as risk-averse preference, the strategy with $\omega<0.5$ as risk-seeking preference, and the strategy with $\omega=0.5$ as risk-neutral preference. To accommodate diverse risk preferences, different values of risk weight factors can be considered. As the weight factor increases from 0 to 1, the scheduling preference turns from risk seeking to risk aversion.

2) Constraint-based Risk Management for CESs

For the essential requirement of CESs, the indoor temperature and the ramping rates of buildings should be maintained within the comfort range, which are expressed as:

$$T^{\min}\leq T_{t,n}\leq T^{\max} \tag{53}$$

$$-\Delta T\leq T_{t,n}-T_{t-1,n}\leq\Delta T \tag{54}$$

Due to the unpredictability of outage duration time, the fault recovery schedule will keep consistent for each possible duration. Therefore, the schedules including charging-discharging power of thermal storage, building temperature in dispersive CESs, and reconfiguration topology for PDN, as well as the load restoration state, will be issued to the local control system for execution.

IV. Solution Methodology of Decentralized Risk-based Self-healing Scheduling

Since PDN and CES usually belong to different entities, only restricted operation information can be exchanged with each other, resulting in the absurdity of centralized scheduling.

In this section, a decentralized method is introduced to achieve private information preserving and independent operation of each subsystem through adaptive ADMM algorithm.

A. Consensus-based ADMM Model for Load Restoration

The energy system is divided into PDN and CES subsystems. The fault restoration of each subsystem is carried out independently, and each operator has complete information of itself, and the shared information with others is only the active and reactive injections for PDN.

In this case, consensus variables $\boldsymbol{Z}_p$ and $\boldsymbol{Z}_q$ are introduced to describe the boundary parameters between them, as depicted in (55).

$$\begin{cases} \boldsymbol{P}_{\mathrm{e}}=\boldsymbol{Z}_p \\ \boldsymbol{Z}_p=\boldsymbol{P}_{\mathrm{ces}} \\ \boldsymbol{Q}_{\mathrm{e}}=\boldsymbol{Z}_q \\ \boldsymbol{Z}_q=\boldsymbol{Q}_{\mathrm{ces}} \end{cases} \tag{55}$$

1) Subproblem of PDN Operation

The augmented Lagrangian function is constructed for the load restoration of PDN subproblem, as expressed in (56) and (57):

$$\begin{aligned} \min \Bigg\{ & (1-\omega)\sum_{t=1}^{t_{\mathrm{out}}} p_t E^{\mathrm{E}} L_t^{\mathrm{E,NS}} \Delta t + \omega\left(\zeta + \frac{1}{1-\varphi}\sum_{t=t_{\mathrm{in}}+\Delta t}^{t_{\mathrm{out}}} p_t \pi_t\right) + \\ & \boldsymbol{\lambda}_{\mathrm{e},p}^k(\boldsymbol{P}_{\mathrm{e}}^k - \boldsymbol{Z}_p^{k-1}) + \frac{\rho}{2}\left\| \boldsymbol{P}_{\mathrm{e}}^k - \boldsymbol{Z}_p^{k-1} \right\|_2^2 + \\ & \boldsymbol{\lambda}_{\mathrm{e},q}^k(\boldsymbol{Q}_{\mathrm{e}}^k - \boldsymbol{Z}_q^{k-1}) + \frac{\rho}{2}\left\| \boldsymbol{Q}_{\mathrm{e}}^k - \boldsymbol{Z}_q^{k-1} \right\|_2^2 \Bigg\} \end{aligned} \tag{56}$$

s.t.

$$(4), (5), (8)\text{-}(14), (35)\text{-}(41) \tag{57}$$

2) Subproblem of CES Operation

The augmented Lagrangian function for CES n is expressed as:

$$\begin{aligned} \min \Bigg\{ & (1-\omega)\sum_{t=1}^{t_{\mathrm{out}}} p_t E^{\mathrm{C}} \left| T_{t,n} - T_{\mathrm{ref}} \right| C_{\mathrm{air}} \rho_{\mathrm{air}} V_n + \\ & \boldsymbol{\lambda}_{\mathrm{ces},p,n}^k(\boldsymbol{P}_{\mathrm{ces},n}^k - \boldsymbol{Z}_{p,n}^{k-1}) + \frac{\rho}{2}\left\| \boldsymbol{P}_{\mathrm{ces},n}^k - \boldsymbol{Z}_{p,n}^{k-1} \right\|_2^2 + \\ & \boldsymbol{\lambda}_{\mathrm{ces},q,n}^k(\boldsymbol{Q}_{\mathrm{ces},n}^k - \boldsymbol{Z}_{q,n}^{k-1}) + \frac{\rho}{2}\left\| \boldsymbol{Q}_{\mathrm{ces},n}^k - \boldsymbol{Z}_{q,n}^{k-1} \right\|_2^2 \Bigg\} \end{aligned} \tag{58}$$

s.t.

$$(17)\text{-}(27), (29)\text{-}(34), (42) \tag{59}$$

The combination of $\boldsymbol{\lambda}_{\mathrm{ces},p,n}/\boldsymbol{\lambda}_{\mathrm{ces},q,n}$ for multiple CESs will form vectors $\boldsymbol{\lambda}_{\mathrm{ces},p}/\boldsymbol{\lambda}_{\mathrm{ces},q}$.

With the consensus-based ADMM algorithm, the unified self-healing model can be decomposed into several subproblems, which can be solved separately by consensus interaction.

The consensus-based ADMM for decentralized recovery is illustrated in Algorithm 1.

Algorithm 1: consensus-based ADMM for decentralized recovery

1. Input parameters for each subsystem, including system topology, load, environment information, and equipment parameters

2. Initialize algorithm parameters, including $\boldsymbol{\lambda}_{\mathrm{e},p}^0$, $\boldsymbol{\lambda}_{\mathrm{e},q}^0$, $\boldsymbol{\lambda}_{\mathrm{ces},p}^0$, $\boldsymbol{\lambda}_{\mathrm{ces},q}^0$, $\boldsymbol{Z}_p^0$, $\boldsymbol{Z}_q^0$, ρ, convergence thresholds $\varepsilon_{\mathrm{pri}}$, $\varepsilon_{\mathrm{dual}}$, and the maximum iteration $k_{\max}$

3. for $k=1, 2, \ldots, k_{\max}$

4. Perform decentralized self-healing optimization for each subsystem

PDN optimization

Objective function: (56)

Constraints: (4), (5), (8)-(14), (35)-(41)

CES optimization

Objective function: (58)

Constraints: (17)-(27), (29)-(34), (42)

5. Exchange coupling variables and update consensus variables:

$$\boldsymbol{Z}_p^k=(\boldsymbol{P}_{\mathrm{e}}^k+\boldsymbol{P}_{\mathrm{ces}}^k)/2,\ \boldsymbol{Z}_q^k=(\boldsymbol{Q}_{\mathrm{e}}^k+\boldsymbol{Q}_{\mathrm{ces}}^k)/2$$

6. Calculate the primal residual PR^k and dual residual DR^k:

$$\begin{gathered} PR_p^k=\left\| \boldsymbol{P}_{\mathrm{e}}^k-\boldsymbol{P}_{\mathrm{ces}}^k \right\|_2^2 \\ PR_q^k=\left\| \boldsymbol{Q}_{\mathrm{e}}^k-\boldsymbol{Q}_{\mathrm{ces}}^k \right\|_2^2 \\ DR_p^k=\left\| \boldsymbol{P}_{\mathrm{e}}^k-\boldsymbol{P}_{\mathrm{e}}^{k-1} \right\|_2^2, \\ DR_q^k=\left\| \boldsymbol{Q}_{\mathrm{e}}^k-\boldsymbol{Q}_{\mathrm{e}}^{k-1} \right\|_2^2 \\ PR^k=\max\{PR_p^k,\ PR_q^k\} \\ DR^k=\max\{DR_p^k,\ DR_q^k\} \end{gathered}$$

7. Check the stopping criteria

if $PR^k \le \varepsilon_{\mathrm{pri}}$ & $DR^k \le \varepsilon_{\mathrm{dual}}$

Output the self-healing scheduling results and break

else

Update the Lagrangian multipliers for each subsystem

$$\begin{gathered} \boldsymbol{\lambda}_{\mathrm{e},p}^{k+1}=\boldsymbol{\lambda}_{\mathrm{e},p}^k+\rho(\boldsymbol{P}_{\mathrm{e}}^k-\boldsymbol{Z}_p^k) \\ \boldsymbol{\lambda}_{\mathrm{e},q}^{k+1}=\boldsymbol{\lambda}_{\mathrm{e},q}^k+\rho(\boldsymbol{Q}_{\mathrm{e}}^k-\boldsymbol{Z}_q^k) \\ \boldsymbol{\lambda}_{\mathrm{ces},p}^{k+1}=\boldsymbol{\lambda}_{\mathrm{ces},p}^k+\rho(\boldsymbol{P}_{\mathrm{ces}}^k-\boldsymbol{Z}_p^k) \\ \boldsymbol{\lambda}_{\mathrm{ces},q}^{k+1}=\boldsymbol{\lambda}_{\mathrm{ces},q}^k+\rho(\boldsymbol{Q}_{\mathrm{ces}}^k-\boldsymbol{Z}_q^k) \end{gathered}$$

8. $k=k+1$

9. end

B. Self-adaptive Step Size Model for ADMM

The convergence efficiency of ADMM is significantly affected by the value of step size. Conventional ADMM is conducted with fixed value, leading to the deterioration of algorithm performance in the last stage of iteration. One effective method to facilitate convergence speed is to adjust parameters for each iteration. As for the issue, a self-adaptive step size method for ADMM (adaptive ADMM) is utilized to improve the algorithm performance, in which the penalty parameter ρ is dynamically modified with less dependence on the initial value, shown as follows [50]:

$$\rho^{k+1}=\begin{cases} \rho^k(1+\mu) & PR^k \ge \sigma\cdot DR^k \\ \rho^k(1+\mu)^{-1} & DR^k \ge \sigma\cdot PR^k \\ \rho^k & \text{others} \end{cases} \tag{60}$$

where $\sigma>1$ and $\mu>1$.

Based on the energy structure and forecasting data of the whole system, the EMSs for CESs and the distribution network operator (DSO) for PDN generate self-governed schedules separately after evaluating the outage duration probability in case of power disruption. The optimal risk-based self-healing strategy for PDN and CESs can be obtained in a decentralized way by limited information exchange and iterative optimization. Then, the corresponding schedules will be issued to each device for execution. The proposed self-healing framework provides a novel decentralized risk-based load recovery for PDN by uncertainty evaluation and CVaR-based management, and the flexibilities of CESs are fully utilized with the self-healing capacity significantly facilitated.

V. Case Studies

In this section, the rationality and effectiveness of the decentralized self-healing strategy with risk management are verified on the distribution network, which is composed of a modified IEEE 33-bus PDN integrated with multiple CESs. Case studies are carried out on Intel CPU i9-10900K and 32 GB RAM-based PC with MATLAB 2020b platform. The self-healing strategy is solved in YALMIP toolbox and optimized by linking CPLEX 12.1 solver [51].

The structure of the modified IEEE 33-bus PDN with multiple CESs is shown in Fig. 1, and the configuration and energy flows of CESs are shown in Fig. 2. The rated voltage of IEEE 33-bus PDN is 12.66 kV and the allowed voltage fluctuation range during outage period is [0.95, 1.05]p. u.. The network consists of 32 lines and 5 tie switches. The total active and reactive loads are 3715.0 kW and 2300 kvar, respectively. Detailed parameters can be found in [52]. Two CESs are installed at nodes 14 and 21 to serve as integrated energy aggregators for providing thermal demands for close-by consumers. Consistent configurations are assumed for all CESs and they are comprised of HPs, WCs, CWTs, GTs and ACs. The device parameters of CESs are listed in Appendix A Table AI. And the converter capacity for each CES is set to be 1500 kVA. The building parameters of each CES are shown in Appendix A Table AII.

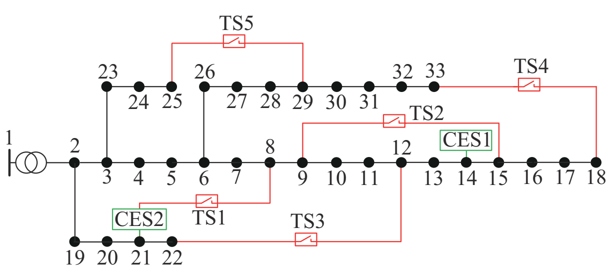

Fig. 1. Structure of modified IEEE 33-bus PDN with multiple CESs.

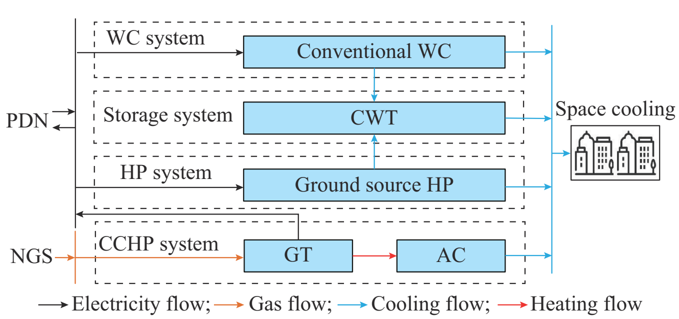

Fig. 2. Configuration and energy flows of CESs.

The scheduling interval is 0.5 hour and a typical day in cooling season is selected for case analysis. The electricity load profile of PDN and the outdoor temperature for the typical cooling day are presented in Fig. 3. To guarantee comfort energy supply for building thermal demand, the indoor temperatures of buildings can vary between 19 ℃ and 25 ℃, of which the standard temperature is 22 ℃. The ramping value of indoor temperature between adjacent intervals cannot exceed 3 ℃. Air specific heat capacity and density are 1.007 kJ/(kg·℃) and 1.2 kg/m^3, respectively.

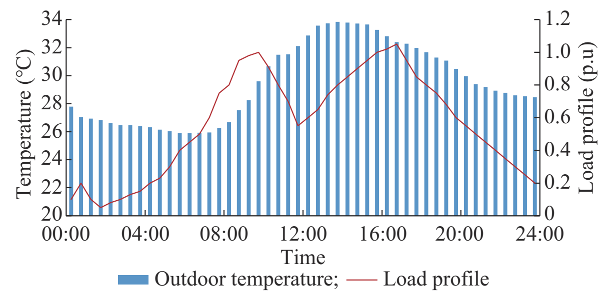

Fig. 3. Electricity load profile of PDN and outdoor temperature for typical cooling day.

The duration of electricity disruption can be 2, 2.5, 3, 3.5, and 4 hours, and the probability of the corresponding scenarios are 0.15, 0.2, 0.3, 0.2, and 0.15, respectively. Thus, the comprehensive probabilities of each period during 02:00-04:00 are 0.333, 0.283, 0.217, 0.117, and 0.050, respectively. Unit penalty costs of curtailed electricity loads in PDN and cooling loads in CESs are 100 CNY/kWh and 5 CNY/kWh, respectively. For risk management parameters, the confidence level α is set to be 0.8. As for the weight factor ω, it can be changed from 0 to 1; and lower value denotes risk-seeking schedule, while higher value represents risk-averse schedule. Especially, 0.7 is assigned to ω for concrete analysis.

In the ADMM optimization procedure, the initial penalty parameter is set to be 1.0. Step size adjustment parameter μ is set to be 2, where the coefficient ν is 6. The maximum iteration is supposed to be 200 and convergence thresholds of both primary and dual residuals are set to be 0.5. For CPLEX solver, it is implemented with default settings and the optimality gap is 1×10^{-4}.

It is assumed that line 1-2 has a permanent three-phase fault at 09:30, and loads of bus 2 to bus 33 are completely out of service. After fault isolation, the risk-based decentralized self-healing operation is conducted for fault restoration.

A. Decentralized Self-healing Scheduling with Consensus-based ADMM

1) Analysis of Self-healing Scheduling Results

The reconfiguration strategy of PDN during 09:30-13:00 is presented in Fig. 4, and the active and reactive power control strategy of GTs in multi-zone CESs is shown in Fig. 5. On behalf of the buses that are fully and partly restored, they are marked with black and green solid circles, respectively, while others are indicated by the hollow ones. Similarly, the green solid rectangle indicates that the CES is chosen as the voltage reference point in the formed island; and the control strategy of the GT in the corresponding CES turns into V/f mode. It can be observed that only one island is formed, and CES2 is picked out to support the network voltage.

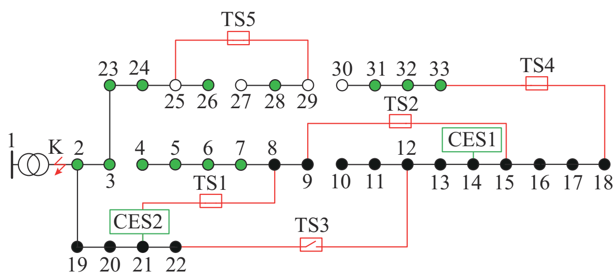

Fig. 4. Reconfiguration strategy of PDN during 09:30-13:00.

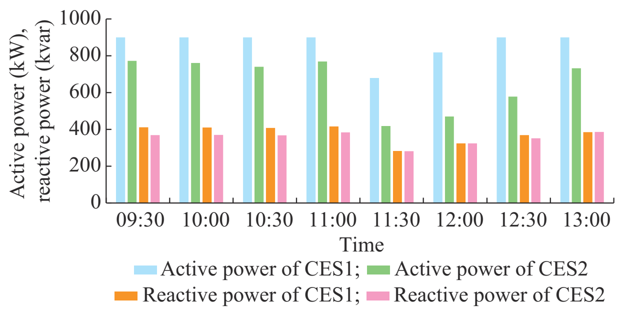

Fig. 5. Active and reactive power control strategy of GTs in multi-zone CESs.

The variation of indoor temperature of buildings in multiple CESs is depicted in Fig. 6. It can be observed that indoor temperature fluctuates within the comfort range and the values are generally near the maximum value. Thus, less cooling energy is needed on the premise of risk controllability, which will contribute to the supply recovery for distribution network.

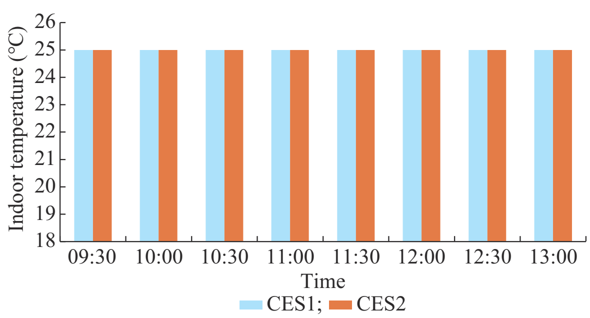

Fig. 6. Indoor temperature of buildings in multiple CESs.

Figure 7 illustrates the stored energy variation of thermal storages in CESs. The positive value of cooling-storage power means that it is in cooling-storage mode; otherwise, it is in cooling-releasing mode. As observed from Fig. 7, the energy storage and release behaviors are conducted timely for responding to the emergency according to the comprehensive risk-based tradeoff of demand profiles between PDN and CESs, as well as the serviceability and coordination of energy supply and storage devices. And the stored energy is released absolutely with no energy redundancy at the end of the maximum outage duration for better restoration effect in multiple possible scenarios.

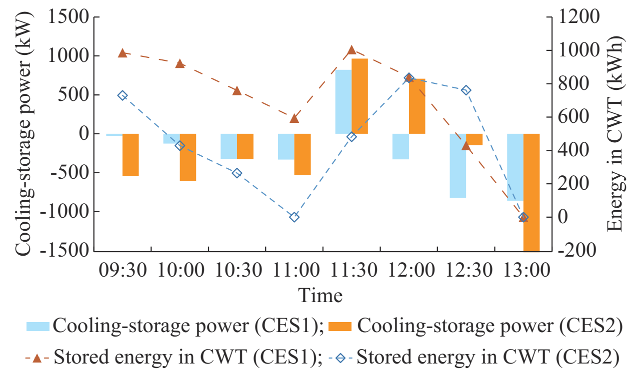

Fig. 7. Stored energy variation of thermal storages in CESs.

Benefiting from flexibilities of multi-area CESs, including the active/reactive support, thermal storage, and building demand response, as well as the flexible topology in PDN, more regulation capacities are exploited and the out-of-service demands can be recovered as much as possible with considering risk preferences. Self-healing oriented fault restoration results of PDN for different outage durations are listed in Table I. The expected unsupplied load is 3985.8 kWh, which is far below the original out-of-service expectation 8555.7 kWh; and the expected restoration rate is 53.4%. Incorporating restoration results of various durations, we can draw that the self-healing strategy can achieve better service recovery effect with the support of regulation potential from CESs.

TABLE I
SELF-HEALING ORIENTED FAULT RESTORATION RESULTS FOR DIFFERENT OUTAGE DURATIONS

Outage duration (hour)	Total load (kWh)	Unrecovered load (kWh)
2.0	6334.1	3026.0
2.5	7355.7	3499.2
3.0	8470.2	3972.0
3.5	9677.6	4444.9
4.0	11052.1	5009.8

2) Comparison of Different Potential Combinations in CESs

Different resource utilization can affect the fault restoration effects significantly. The comparison of different potential combination scenarios for CESs is depicted in Table II.

TABLE II
COMPARISON OF DIFFERENT POTENTIAL COMBINATION SCENARIOS FOR CESS

Scenario	Thermal storage	Building thermal inertia	Expected loss of PDN (kWh)
1	×	√	4155.0
2	√	×	4764.9
3	√	√	3985.8

Note: √ means with consideranion and × means without consideranion.

Compared with scenario 1, the thermal storage devices, i.e., CWTs, are considered in scenario 3. With timely energy charging-discharging behaviors of CWTs, additional flexibilities are provided for spatio-temporal emergency response in case of power disruption. Thus, more out-of-service loads are recovered with the risk-based self-healing strategy.

In scenario 2, the thermal inertia of building in CESs is ignored in contrast with scenario 3. By considering building thermal inertia, the indoor temperature can be regulated within reasonable range along with more adjustable margin for energy coordination and multi-area complementation. And the load recovery effect can be effectively improved.

By comparing the results of different potential combinations, it can be noted that the self-healing strategy can fully exploit the regulation potentials from CESs for facilitating self-healing capacity, achieving better fault restoration effect.

3) Performance Analysis of Adaptive ADMM

To indicate the effectiveness of the proposed decentralized strategy, the convergence processes of primary and dual residuals for adaptive and standard ADMM are illustrated in Fig. 8. It is observed that the consensus-based ADMM with self-adaptive step size converges by 74 iterations, whereas the primary and dual residuals of standard ADMM cannot converge to the set thresholds in 200 iterations. The step size of adaptive ADMM is dynamically updated during each iteration after the evaluation of primary and dual residuals, realizing a significant acceleration of convergence performance.

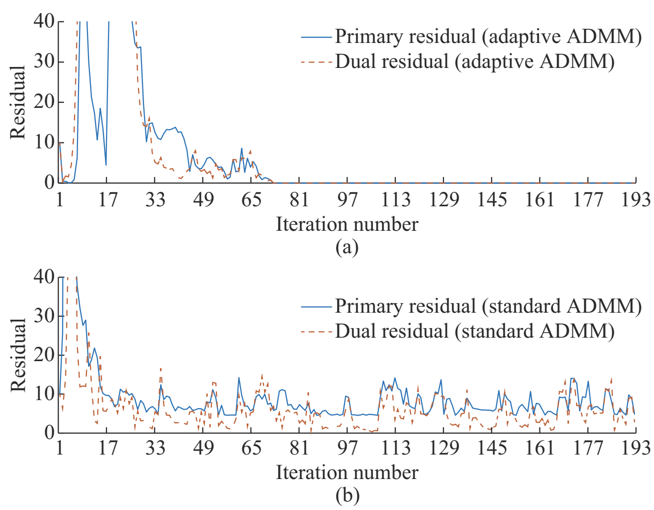

Fig. 8. Convergence processes of primary and dual residuals for adaptive and standard ADMM. (a) Residual convergence for adaptive ADMM. (b) Residual convergence for standard ADMM.

To further demonstrate the accuracy of the decentralized strategy, the restoration results of conventional centralized and adaptive ADMM are shown in Table III. The gap of expected total load loss (in goal function) of PDN and CESs for centralized and decentralized strategies is very small; thus, the validity of the decentralized strategy is verified. Although more computational time is needed for iteration optimization, the privacy protection and nearby optimal solution are realized with moderate solution time. Therefore, it is more applicable to actual energy systems with various entities.

TABLE III
RESTORATION RESULTS OF CONVENTIONAL CENTRALIZED AND ADAPTIVE ADMM

ADMM	Expected loss of PDN (kWh)	Expected loss of CESs (kWh)	Optimal goal (CNY)	Solution time (s)
Centralized	3029.7	2416.8	129248.2	60.4
Adaptive	3030.9	2416.8	129262.6	1771.0

B. Risk-based Management Analysis for Service Recovery

1) Impact Analysis of Weight Factor

The variation profiles of load loss value and CVaR with different weight factors are presented in Fig. 9.

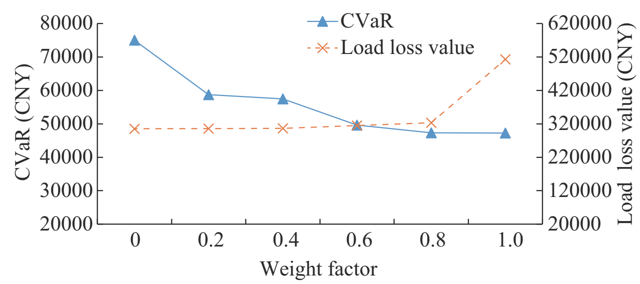

Fig. 9. Load loss value and CVaR with different weight factors.

As can be observed, with the increase of weight factor, the CVaR decreases while the expected load loss value increase simultaneously; and system operation varies from risk-seeking to risk-averse preferences. In other words, the lower operation risk can be obtained along with poorer fault-restoration effect, and vice versa. In actual operation, the operator needs to select the appropriate weight factor to pursue the utmost service restoration on the premise of satisfying their specific risk preference.

Without loss of generality, the operation results with different weight factors of 0.2, 0.6, and 1.0 are listed in Table IV, and the corresponding schedules of CES1 with different weight factors are shown in Fig. 10.

TABLE IV
OPERATION RESULTS WITH DIFFERENT WEIGHT FACTORS

Value of weight factor	Load loss value (CNY)	CVaR (CNY)
0.2	305723.7	58736.0
0.6	314580.8	49620.4
1.0	512733.0	47237.3

It is obvious that the risk-seeking strategy (Fig. 10(a)) tries its best to recover load and the initial stored energy in CWTs is released directly for supporting the power demand in PDN. As for risk-averse strategy (Fig. 10(b) and Fig. 10(c)), the energy storage and release behaviors exist simultaneously for the trade-off between load loss and risk values. The stronger willing for risk aversion, the more energy will be reserved for vigorous risk management under uncertain outage duration. With time-series energy transfer by storages and complementation coordination of coupling devices in CESs, as well as the flexible regulation in PDN, different risk management schedules can be generated by reasonably setting the weight factors based on the operator's preference on the original target and risk values.

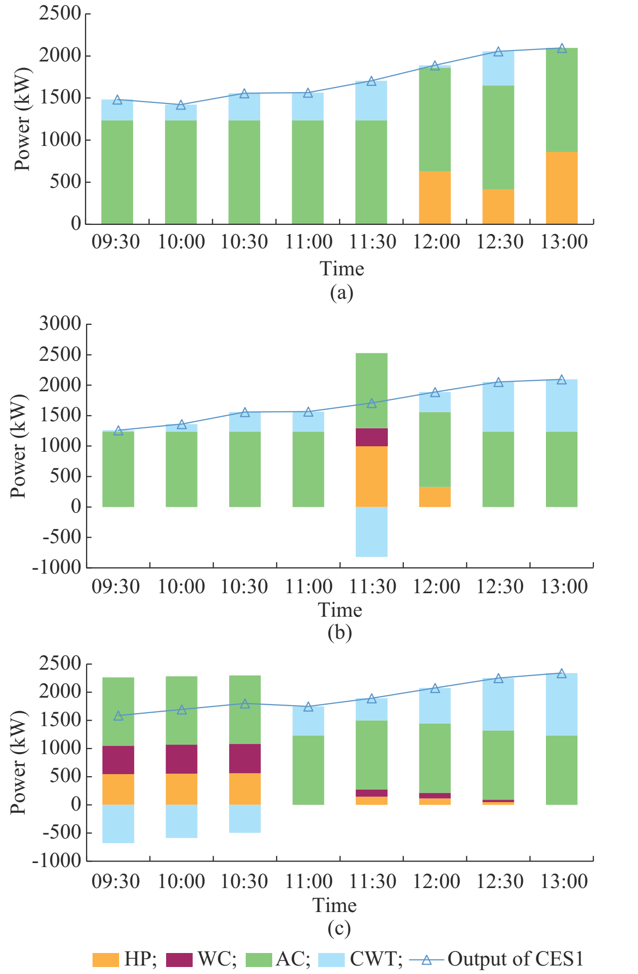

Fig. 10. Schedules of CES1 with different weight factors. (a) Operation state of CES1 when $\omega=0.2$. (b) Operation state of CES1 when $\omega=0.6$. (c) Operation state of CES1 when $\omega=1.0$.

2) Analysis of Different Self-healing Schemes

To further demonstrate the effectiveness of risk management strategy, three schemes are constructed for performance comparison.

1) Scheme 1: the proposed strategy, i.e., CVaR-based self-healing scheduling, is adopted for service restoration.

2) Scheme 2: the stochastic optimization is conducted for service restoration, i.e., multiple scenarios with risk weight factor $\omega=0$.

3) Scheme 3: the deterministic operation for the worst-case scenario is conducted for service restoration, i.e., the outage duration time is 4 hours.

The variations of stored energy in CWTs for different schemes are shown in Fig. 11, and Fig. 12 illustrates the unrecovered load of PDN for each scheduling period. Compared with Scheme 3, the thermal energies are released more rapidly for Scheme 2 due to large probability weight of the initial few periods. As for Scheme 1, energy-releasing behaviors occur at both head and tail intervals for recovery purposes; and energy-storage behaviors appear during middle periods to support emergency energy demand with risk management, especially for the last two intervals.

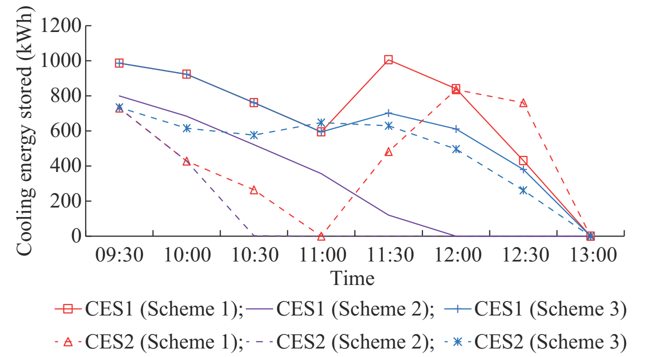

Fig. 11. Variation of stored energy in CWTs for different schemes.

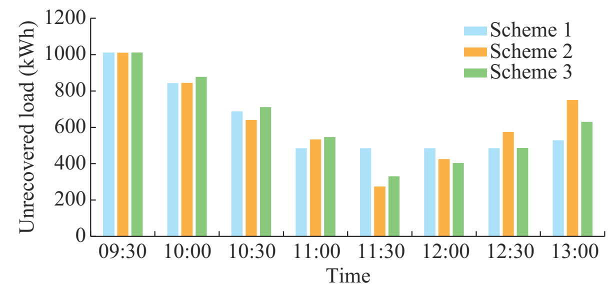

Fig. 12. Unrecovered load of PDN for each scheduling period.

Incorporating Fig. 12, it can be observed the out-of-service amount in the last few intervals of Scheme 1 is much less than Schemes 2 and 3, achieving better risk management while balancing the total load loss.

The comparisons of operation results for different schemes are listed in Table V. As can be observed, the load restoration of Scheme 3 is over-conservative, and the load loss value is the most severe in all schemes. The stochastic optimization in Scheme 2 has the lowest loss value and the highest CVaR, resulting in significant load-shedding risks in actual operation. As for Scheme 1, the best risk management performance is obtained with a moderate load loss value. Thus, it can be concluded that the risk-based self-healing strategy can conduct an effective load recovery with strong risk adaptability for uncertain outage duration.

TABLE V
OPERATION RESULTS FOR DIFFERENT SCHEMES

Scheme	CVaR (CNY)	Load loss value (CNY)
1	49617.1	314582.5
2	74994.0	305358.4
3	62955.0	316728.4

VI. CONCLUSION

This paper presents a decentralized risk-based self-healing strategy for PDN. The regulation potentials of multiple CESs, including active and reactive power support of GTs, as well as emergency response of thermal storage and building thermal inertia, are fully utilized for load restoration in case of power disruption. In terms of inherent outage duration uncertainty, bilateral risk management with CVaR for PDN and essential constraints for CESs is implemented for operation analysis considering risk preference. Furthermore, an adaptive ADMM is introduced to achieve decentralized optimization.

Case studies are conducted using the modified IEEE 33-bus PDN with multi-point CESs. It is indicated that the strategy can give full play to the flexible support capacities of multiple resources in CESs to restore out-of-service loads as much as possible. By applying bilateral risk measures with CVaR, the PDN load shedding of each period can be reasonably coordinated for effective operational risk control, guaranteeing the indispensable supply of CESs. Besides, the consensus-based ADMM solution is carried out to conduct decentralized optimal scheme of PND and CESs. The results are in accordance with that of the centralized strategy, and limited information interaction and privacy protection can be achieved. With the application of adaptive ADMM, convergence performances can be effectively improved.

In conclusion, the proposed risk-based decentralized self-healing strategy can realize better emergency service recovery, with tough risk management ability under unpredictable outage duration. And the decentralized strategy is more applicable for privacy-safety scheduling under the independent operation of subsystems.

APPENDIX A

TABLE AI
DEVICE PARAMETERS OF CESs

Item	Capacity	COP or efficiency	Loss rate
HP	1000 kW for CES1 1000 kW for CES2	5.38	0.001
WC	1000 kW for CES1 1000 kW for CES2	5.13	
CWT	10000 kWh for CES1 15000 kWh for CES2		
GT	900 kW for CES1 800 kW for CES2	0.35 for electricity 0.40 for heating	
AC	1200 kW for CES1 1000 kW for CES2	1.20	

TABLE AII
BUILDING PARAMETERS IN EACH CES

location	Surface area (m^2)	Volume (m^3)	Dissipation coefficient ($W/(m^2\cdot{}^\circ C)$)
CES1	200000	280000	1.2
CES2	250000	320000	1.2

REFERENCES

[1] M. A. Bagherian and K. Mehranzamir, "A comprehensive review on renewable energy integration for combined heat and power production," *Energy Conversion and Management*, vol. 224, p. 113454, Nov. 2020.

[2] L. Chen, Q. Xu, Y. Yang *et al.*, "Community integrated energy system trading: a comprehensive review," *Journal of Modern Power Systems and Clean Energy*, vol. 10, no. 6, pp. 1445-1458, Nov. 2022.

[3] C. Lv, H. Yu, P. Li *et al.*, "Coordinated operation and planning of integrated electricity and gas community energy system with enhanced operational resilience," *IEEE Access*, vol. 8, pp. 59257-59277, Mar. 2020.

[4] A. Ghanbari, H. Karimi, and S. Jadid, "Optimal planning and operation of multi-carrier networked microgrids considering multi-energy hubs in distribution networks," *Energy*, vol. 204, p. 117936, Aug. 2020.

[5] X. Zhang, C. Liang, M. Shahidehpour *et al.*, "Reliability-based optimal planning of electricity and natural gas interconnections for multiple energy hubs," *IEEE Transactions on Smart Grid*, vol. 8, no. 4, pp. 1658-1667, Jul. 2017.

[6] D. Feng, F. Wu, Y. Zhou *et al.*, "Multi-agent-based rolling optimization method for restoration scheduling of distribution systems with distributed generation," *Journal of Modern Power Systems and Clean Energy*, vol. 8, no. 4, pp. 737-749, Jul. 2020.

[7] A. A. Bajwa, H. Mokhlis, and S. Mekhilef, "Enhancing power system resilience leveraging microgrids: a review," *Journal of Renewable and Sustainable Energy*, vol. 11, no. 3, p. 035503, Apr. 2019.

[8] S. Poudel and A. Dubey, "Critical load restoration using distributed energy resources for resilient power distribution system," *IEEE Transactions on Power Systems*, vol. 34, no. 1, pp. 52-63, Jul. 2018.

[9] F. Shen, Q. Wu, and Y. Xue, "Review of service restoration for distribution networks," *Journal of Modern Power Systems and Clean Energy*, vol. 8, no. 1, pp.1-14, Jan. 2019.

[10] E. Hossain, S. Roy, N. Mohammad *et al.*, "Metrics and enhancement strategies for grid resilience and reliability during natural disasters," *Applied Energy*, vol. 290, p. 116709, May 2021.

[11] Y. Li, J. Xiao, C. Chen *et al.*, "Service restoration model with mixed-integer second-order cone programming for distribution network with distributed generations," *IEEE Transactions on Smart Grid*, vol. 10, no. 4, pp. 4138-4150, Jul. 2018.

[12] J. Jian, P. Li, H. Yu *et al.*, "Multi-stage supply restoration of active distribution networks with SOP integration," *Sustainable Energy, Grids and Networks*, vol. 29, p. 100562, Mar. 2022.

[13] H. Ji, C. Wang, P. Li *et al.*, "SOP-based islanding partition method of active distribution networks considering the characteristics of DG, energy storage system and load," *Energy*, vol. 155, pp. 312-325, Jul. 2018.

[14] H. Zhao, Z. Lu, L. He *et al.*, "Two-stage multi-fault emergency rush repair and restoration robust strategy in distribution networks," *Electric Power Systems Research*, vol. 184, p. 106335, Mar. 2020.

[15] J. Liu, C. Qin, and Y. Yu, "A comprehensive resilience-oriented FLISR method for distribution systems," *IEEE Transactions on Smart Grid*, vol. 12, no. 3, pp. 2136-2152, May 2021.

[16] X. Liu, H. Wang, Q. Sun *et al*., "Research on fault scenario prediction and resilience enhancement strategy of active distribution network under ice disaster," *International Journal of Electrical Power & Energy Systems,* vol. 135, p. 107478, Feb. 2022.

[17] Y. Wang, Y. Xu, J. He *et al.*, "Coordinating multiple sources for service restoration to enhance resilience of distribution systems," *IEEE Transactions on Smart Grid*, vol. 10, no. 5, pp. 5781-5793, Sept. 2019.

[18] F. Hafiz, B. Chen, C. Chen *et al.*, "Utilising demand response for distribution service restoration to achieve grid resiliency against natural disasters," *IET Generation, Transmission and Distribution*, vol. 13, no. 14, pp. 2942-2950, Jul. 2019.

[19] X. Wang, X. Li, X.-J. Li *et al*., "Soft open points based load restoration for the urban integrated energy system under extreme weather events," *IET Energy Systems Integration,* vol. 4, pp. 335-350, Feb. 2022.

[20] F. Vazinram, M. Hedayati, R. Effatnejad *et al.*, "Self-healing model for gas-electricity distribution network with consideration of various types of generation units and demand response capability," *Energy Conversion and Management*, vol. 206, p. 112487, Feb. 2020.

[21] C. Li, P. Li, H. Yu *et al.*, "Optimal planning of community integrated energy station considering frequency regulation service," *Journal of Modern Power Systems and Clean Energy*, vol. 9, no. 2, pp. 264-273, Mar. 2021.

[22] M. Yan, Y. He, M. Shahidehpour *et al.*, "Coordinated regional-district operation of integrated energy systems for resilience enhancement in natural disasters," *IEEE Transactions on Smart Grid*, vol. 10, no. 5, pp. 4881-4892, Sept. 2019.

[23] C. Wang, W. Wei, J. Wang *et al.*, "Robust defense strategy for gas-electric systems against malicious attacks," *IEEE Transactions on Power Systems*, vol. 32, no. 4, pp. 2953-2965, Jul. 2016.

[24] H. Cong, Y. He, X. Wang *et al.*, "Robust optimization for improving resilience of integrated energy systems with electricity and natural gas infrastructures," *Journal of Modern Power Systems and Clean Energy*, vol. 6, no. 5, pp. 1066-1078, Sept. 2018.

[25] X. Li, X. Du, T. Jiang T *et al.*, "Coordinating multi-energy to improve urban integrated energy system resilience against extreme weather events," *Applied Energy*, vol. 309, p. 118455, Mar. 2022.

[26] C. Shao, M. Shahidehpour, X. Wang *et al.*, "Integrated planning of electricity and natural gas transportation systems for enhancing the power grid resilience," *IEEE Transactions on Power Systems*, vol. 32, no. 6, pp. 4418-4429, Nov. 2017.

[27] C. Lv, R. Liang, W. Jin *et al.*, "Multi-stage resilience scheduling of electricity-gas integrated energy system with multi-level decentralized reserve," *Applied Energy*, vol. 317, p. 119165, Jul. 2022.

[28] X. Jiang, J. Chen, M. Chen *et al.*, "Multi-stage dynamic post-disaster recovery strategy for distribution networks considering integrated energy and transportation networks," *CSEE Journal of Power and Energy Systems*, vol. 7, no. 2, pp. 408-420, Oct. 2020.

[29] R. Hemmati, H. Mehrjerdi, S. M. Nosratabadi, "Resilience-oriented adaptable microgrid formation in integrated electricity-gas system with deployment of multiple energy hubs," *Sustainable Cities and Society*, vol. 71, p. 102946, Aug. 2021.

[30] T. Qian, X. Chen, Y. Xin *et al.*, "Resilient decentralized optimization of chance constrained electricity-gas systems over lossy communication networks," *Energy*, vol. 239, p. 122158, Jan. 2022.

[31] P. Wang, Q. Wu, S. Huang *et al.*, "ADMM-based distributed active and reactive power control for regional AC power grid with wind farms," *Journal of Modern Power Systems and Clean Energy*, vol. 10, no. 3, pp. 588-596, Jun. 2021.

[32] S. Xu, Z. Yan, D. Feng *et al.*, "Decentralized charging control strategy of the electric vehicle aggregator based on augmented Lagrangian method," *International Journal of Electrical Power & Energy Systems*, vol. 104, pp. 673-679, Jan. 2019.

[33] X. Zhou, Q. Ai, and M. Yousif, "Two kinds of decentralized robust economic dispatch framework combined distribution network and multi-microgrids," *Applied Energy*, vol. 253, p. 113588, Nov. 2019.

[34] C. He, L. Wu, T. Liu *et al.*, "Robust co-optimization scheduling of electricity and natural gas systems via ADMM," *IEEE Transactions on Sustainable Energy*, vol. 8, no. 2, pp. 658-670, Apr. 2016.

[35] J. Wei, Y. Zhang, J. Wang *et al.*, "Decentralized demand management based on alternating direction method of multipliers algorithm for industrial park with CHP units and thermal storage," *Journal of Modern Power Systems and Clean Energy*, vol. 10, no. 1, pp. 120-130, Jan. 2022.

[36] N. Jia, C. Wang, W. Wei *et al.*, "Decentralized robust energy management of multi-area integrated electricity-gas systems," *Journal of Modern Power Systems and Clean Energy*, vol. 9, no. 6, pp. 1478-1489, Nov. 2021.

[37] W. Lin, X. Jin, H. Jia *et al*., "Decentralized optimal scheduling for integrated community energy system via consensus-based alternating direction method of multipliers," *Applied Energy*, vol. 302, p. 117448, Nov. 2021.

[38] G. Li, K. Yan, R. Zhang *et al*., "Resilience-oriented distributed load restoration method for integrated power distribution and natural gas systems," *IEEE Transactions on Sustainable Energy*, vol. 13, no. 1, pp. 341-352, Sept. 2021.

[39] X. Xu, W. Hu, W. Liu *et al.*, "Robust energy management for an ongrid hybrid hydrogen refueling and battery swapping station based on renewable energy," *Journal of Cleaner Production*, vol. 331, p. 129954, Jan. 2022.

[40] Z. Li, S. Su, X. Jin *et al*., "Stochastic and distributed optimal energy management of active distribution network with integrated office buildings," *CSEE Journal of Power and Energy Systems*. doi: 10.17775/CSEEJPES

[41] S. Su, Z. Li, X. Jin *et al.*, "Energy management for active distribution network incorporating office buildings based on chance-constrained programming," *International Journal of Electrical Power & Energy Systems*, vol. 134, p. 107360, Jan. 2022.

[42] X. Yu and D. Zheng, "Cross-regional integrated energy system scheduling optimization model considering conditional value at risk," *International Journal of Energy Research*, vol. 44, no. 7, pp. 5564-5581, Jun. 2020.

[43] A. Xuan, X. Shen, Q. Guo *et al.*, "A conditional value-at-risk based planning model for integrated energy system with energy storage and renewables," *Applied Energy*, vol. 294, p. 116971, Jul. 2021.

[44] J. Wang and Y. Song, "Distributionally robust OPF in distribution network considering CVaR-averse voltage security," *International Journal of Electrical Power & Energy Systems*, vol. 145, p. 108624, Feb. 2023.

[45] Z. Liu, S. Liu, Q. Li *et al.*, "Optimal day-ahead scheduling of islanded microgrid considering risk-based reserve decision," *Journal of Modern Power Systems and Clean Energy*, vol. 9, no. 5, pp. 1149-1160, Sept. 2021.

[46] A. S. G. Langeroudi, M. Sedaghat, S. Pirpoor *et al.*, "Risk-based optimal operation of power, heat and hydrogen-based microgrid considering a plug-in electric vehicle," *International Journal of Hydrogen Energy*, vol. 46, no. 58, pp. 30031-30047, Aug. 2021.

[47] J. Zhao, M. Zhang, H. Yu *et al*., "An islanding partition method of active distribution networks based on chance-constrained programming," *Applied Energy*, vol. 242, pp. 78-91, May 2019.

[48] Y. Li, C. Wang, G. Li *et al.*, "Improving operational flexibility of integrated energy system with uncertain renewable generations considering thermal inertia of buildings," *Energy Conversion and Management*, vol. 207, p. 112526, Mar. 2020.

[49] D. Xiao, H. Chen, C. Wei *et al.*, "Statistical measure for risk-seeking stochastic wind power offering strategies in electricity markets," *Journal of Modern Power Systems and Clean Energy*, vol. 10, no. 5, pp. 1437-1442, Sept. 2022.

[50] Z. Li, P. Li, Z. Yuan *et al*, "Optimized utilization of distributed renewable energies for island microgrid clusters considering solar-wind correlation," *Electric Power Systems Research*, vol. 206, p. 107822, May 2022.

[51] IBM. (2022, Dec.). IBM ILOG CPLEX Optimization Studio. [Online]. Available: https://www.ibm.com/products/Ilog-cplex-optimization-studio

[52] P. Li, H. Ji, C. Wang *et al.*, "Coordinated control method of voltage and reactive power for active distribution networks based on soft open point," *IEEE Transactions on Sustainable Energy*, vol. 8, no. 4, pp. 1430-1442, Oct. 2017.

Chaoxian Lv received the B.S. and M.S. degrees in electrical engineering from Hunan University, Changsha, China, in 2011 and 2014, respectively, and the Ph.D. degree in electrical engineering from Tianjin University, Tianjin, China, in 2019. He is currently a Lecturer with the School of Electrical Engineering, China University of Mining and Technology, Xuzhou, China. His current research interests include operation analysis of integrated energy system and active distribution network.

Rui Liang received the B. S. and Ph. D. degrees in electrical engineering from China University of Mining and Technology, Xuzhou, China, in 2001 and 2010, respectively. He is now a Professor in School of Electrical Engineering, China University of Mining and Technology. Since 2020, he has been with the Huaiyin Institute of Technology, Huai'an, China, where he serves as a specially-appointed Professor with the School of Automation. His current research interests include the protection in power grid, critical electrical equipment assessment, and modeling in energy interconnection.

Yuanyuan Chai received the B.S. and Ph.D. degrees in electrical engineering from Tianjin University, Tianjin, China, in 2015 and 2021, respectively. She is currently a Lecturer with with the School of Electrical Engineering, Hebei University of Technology, Tianjin, China. Her current research interests include distributed optimization and power quality improvement in active distribution networks.